

Article

Impact of Climate Change on Spatio-Temporal Distribution of Glaciers in Western Karakoram Region since 1990: A Case Study of Central Karakoram National Park

Muhammad Farhan Ul Moazzam ¹, Jinho Bae ² and Byung Gul Lee ^{1,*}

¹ Department of Civil Engineering, College of Ocean Science, Jeju National University, 102 Jejudaehakro, Jeju 63243, Korea

² Department of Ocean System Engineering, Jeju National University, 102 Jejudaehakro, Jeju 63243, Korea

* Correspondence: leebg@jejunu.ac.kr

Abstract: Glaciers in the Upper Indus Basin (UIB) in Pakistan are the major source of water, irrigation, and power production for downstream regions. Global warming has induced a substantial impact on these glaciers. In the present study, Landsat images were utilized to evaluate the glaciers for the period from 1990–2020 in the Central Karakoram National Park (CKNP) region to further correlate with climate parameters. The results reveal that glaciers are retreating and the highest (2.33 km²) and lowest (0.18 km²) recession rates were observed for Biafo and Khurdopin glaciers, respectively. However, a minor advancement has also been observed for the period from 1990–2001. More than 80% of glacier recession was recorded between 2009–2020 because mean summer temperature increased at both Skardu and Gilgit meteorological stations, while precipitation decreased at both stations from 2005–2020. The increase in mean summer temperature and decrease in winter precipitation resulted in glacial retreat, which will lead to water scarcity in the future as well as affect the agriculture sector and hydropower production in downstream areas of the Indus River basin.

Keywords: Landsat; NDSI; ice and debris; spot 7; temperature; precipitation



Citation: Moazzam, M.F.U.; Bae, J.; Lee, B.G. Impact of Climate Change on Spatio-Temporal Distribution of Glaciers in Western Karakoram Region since 1990: A Case Study of Central Karakoram National Park. *Water* **2022**, *14*, 2968. <https://doi.org/10.3390/w14192968>

Academic Editors: Caterina Samela, Maria Lanfredi, Rosa Coluzzi, Fernando Nardi and Antonio Annis

Received: 8 August 2022

Accepted: 16 September 2022

Published: 21 September 2022

Publisher's Note: MDPI stays neutral with regard to jurisdictional claims in published maps and institutional affiliations.



Copyright: © 2022 by the authors. Licensee MDPI, Basel, Switzerland. This article is an open access article distributed under the terms and conditions of the Creative Commons Attribution (CC BY) license (<https://creativecommons.org/licenses/by/4.0/>).

1. Introduction

The third-largest ice reserve outside the polar regions is made through the largest mountain glacier chain (Hindu-Kush, Karakoram, and Himalaya: HKH) which is the source of water for 1.3 billion people (20% world's population) in the HKH region [1,2] however, global warming has had a substantial impact on glaciers in the region. In the last two decades, glaciers in the Himalayan region retreated extensively [3], although it is still unclear which climatic variable is playing a significant role in glacier retreat. Glaciers are considered the prime source of climate change indicators [4]. The climate of the HKH region varies greatly and depends on two different climate regimes in which westerlies influence the northern and western parts while southern and eastern parts are influenced by monsoon [5]. The largest rivers of Asia, including Brahmaputra, Indus, and the Ganges, are fed by these high mountain glaciers [2]. Glaciers in the HKH region are called the water tower of Asia [6]. These water towers are very important for irrigation, human consumption, and hydropower production [7,8] in the downstream region. The mighty Indus river also receives 80 percent of its water from these glaciers [9].

According to an Intergovernmental panel on climate change (IPCC) (2013) report, the global temperature has increased by 0.85 °C since 1980, and it is expected to reach 3.7 °C by the end of this century. Sabin et al. (2020) [10] reported that the mean annual temperature of the HKH region is showing a fast warming trend since the mid-20th century. Krishnan et al. (2019) [11] noticed that the mean temperature of the HKH region increased at a rate of 0.104 °C/decade during the period from 1901–2014. Fowler and Archer (2006) [8] also examined that precipitation or snowfall has reduced in the winter,

and the mean temperature of the Upper Indus Basin (UIB) region has increased in the summer. Sun et al. (2017) [12] revealed that cold events have decreased and warm events have increased significantly over the HKH region. The same authors observed that warm nights have increased and cold days have decreased significantly since 1990. Thus, this increasing temperature has been affecting the water tower in the UIB more rapidly than in any other part of the world. On the contrary, in the literature, we have also observed that Karakoram glaciers seem stable or have positive mass balance [13] when most of the glaciers in the world are retreating. Hence, this behavior is usually known as a Karakoram anomaly [14]. The anomalous behavior of Karakoram glaciers is due to their response to atmospheric circulation and intensity of the westerly jet [15] or the advantage of supraglacial debris, which can reduce the melting rate [16]. Precipitation in the Karakoram region comes from mid-latitude westerlies in the winter and spring seasons; therefore, it works as an accumulation period for glaciers [17].

Globally, glaciers are retreating and this issue has attracted many research groups to address the correlation between global climate change and the cryosphere. Various studies have concluded that glaciers are retreating globally due to climate change. Shafique et al. (2018) [18] concluded that Batura, Gulkin, Passu, and Gulmit glaciers are retreating over time. The authors also concluded that debris-free glaciers are more prone to climate change compared to debris-covered glaciers. Additionally, Imran and Ahmad (2021) [1] concluded that the Khurdopin glacier surges every 20 years, and 0.69 and 0.63 km² surges were observed in 2000 and 2017, respectively. The authors also observed the 1–4 °C increase in minimum and maximum winter temperature. Mazhar et al. (2020) [19] concluded that the Hispar glacier is retreating at a rate of 1.67 km²/year and, due to warmer temperatures, the glaciers are retreating rather than accumulating. Chowdhury et al. (2021) [20] studied glacier change in the eastern Himalayan region using multi-sensor datasets (Hexagon, Landsat, and Sentinel-2A, Stockholm, Sweden) for the period from 1975–2018. The authors revealed that overall, 17.9 km² of glacier area retreated in the studied period. The authors observed that in the 21st century, the glaciers are retreating much faster compared to the 20th century. Debnath et al. (2019) [21] conducted a detailed study in Changme Khangpu Basin in the Eastern Himalaya region for the period from 1975–2016. Authors delineated 81 glaciers in the region and found that 20% of the glacier area has been lost from the region in the studied period. Kehrwald et al. (2008) [22] concluded that the Naimona Nyi glacier in Tibet has not received any ice accumulation since the mid-19th century. The same authors also reported that in the last 50 years, 80% of glaciers in Western China experienced retreating phenomena. Thus, it is a dire need to monitor glaciers over this time period to analyze the impact of climate change.

For glacier investigation, field campaigns are labor-intensive, expensive, dangerous, and time-consuming due to the remoteness, rugged terrain, and hazardous region that make it difficult to monitor continuously [23]. On the other hand, on-screen, manual digitization of satellite images along with field observation is the most efficient and accurate method but it is also labor-intensive and time-consuming. Alternatively, remote sensing (RS) is a valuable tool for ice and glacier mapping [1,18,23,24]. Through RS, these glaciers can be monitored at regular intervals and it helps to provide a clear picture of glaciers with multitemporal and multispectral data. Therefore, various RS-based indices for ice and snow distribution have been developed to use with multispectral image bands, i.e., normalized difference snow index (NDSI) [24], normalized difference water index (NDWI) [25], normalized difference debris index (NDDI) [26], normalized difference principal component snow index (NDPCSI) [27], and normalized difference snow thermal index (NDSTI) [28]. Among these indices, NDSI has been used in many studies to efficiently detect ice in satellite images because of its satisfactory results with detection in mountain shadows [19,28,29]. Shafique et al. (2018) [18] applied multitemporal Landsat images for glacier mapping using NDSI and compared the results with high-resolution Worldview-2 data and found a 98.57% accuracy in glacier delineation. Burns and Nolin (2014) [30] compared the band ratio with the NDSI method and found that NDSI works best in the detection of ice in the shadowed

region. However, the index is too sensitive to debris-covered glaciers to differentiate it from clean ice [10,29]; therefore, to overcome this problem, Paul et al. (2004) [31] used the slope threshold method and, recently, Debnath et al. (2019) [21] successfully near-accurately delineated clean ice and debris-covered glaciers in Sikkim Himalaya with the help of band ratio and composites maps of LST, slope, and NDSI.

Pandey et al. (2018) [32] visually interpreted the Pindari glacier and its snout position and digitized it using multitemporal Landsat images. Bajracharya et al. (2014) [3] evaluated the glacier changes in Bhutan with object-based image classification assisted by manual editing. Imran and Ahmad (2021) [1] studied the Khurdopin glacier using the normalized snow difference index (NSDI), NDWI, and land use/land cover (LULC) and correlated it with climatic variables. However, in the present study, we investigated the Central Karakoram National Park (CKNP) glaciers (Khurdopin, Biafo, Hispar, Panmah, and Virjerab) (Figure 1). The purpose of selecting the glaciers in the CKNP region is that more than 40% of the area inside the CKNP region is covered by glaciers, and 30% of Pakistan's Karakoram glaciers are in the CKNP region. To investigate the melting ice in the CKNP region, we used NDSI and the slope threshold method for the temporal period from 1990 to 2020 using Landsat satellite data, and we also estimated the changes within glaciers (ice and debris) and correlate them to precipitation and temperature.

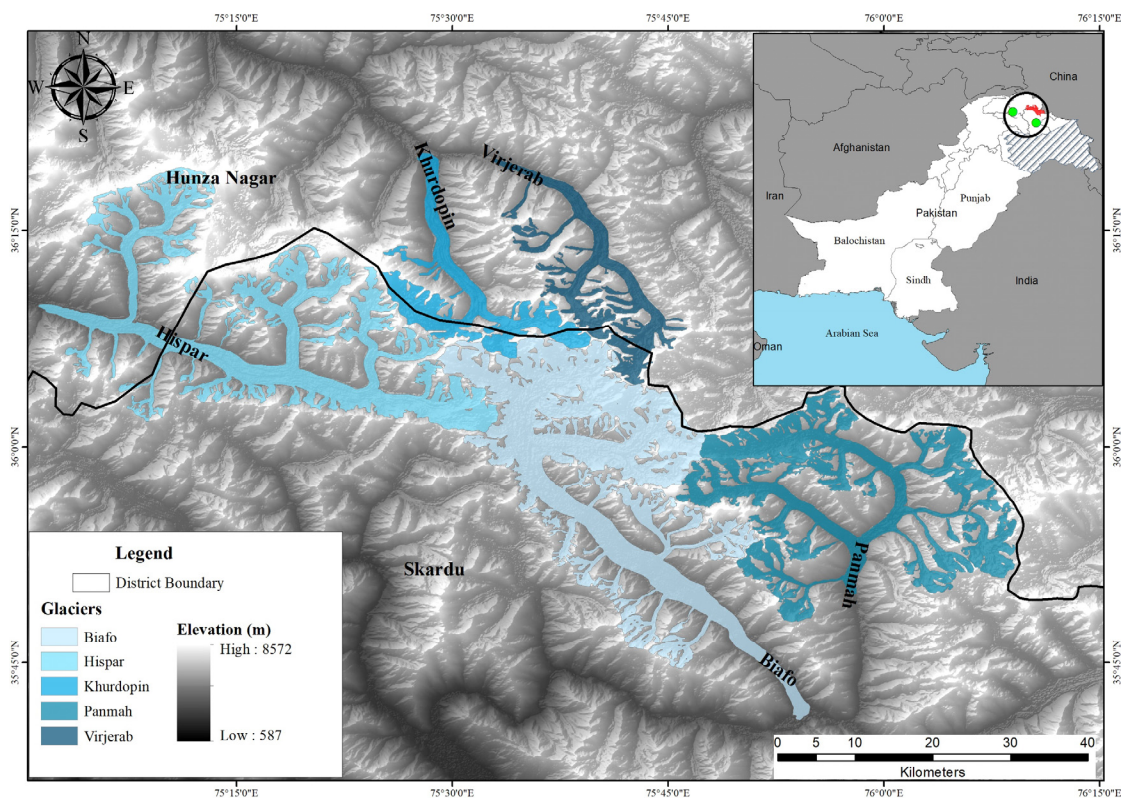


Figure 1. Location map of the Central Karakoram National Park (CKNP) in Gilgit Baltistan. Glacier boundaries are shown on ASTER 30-m GDEM. The red color boundary inside the encircled area shows the studied area and green dots show the location of Gilgit and Skardu meteorological stations in Gilgit Baltistan.

Study Area

The HKH region is spread over 2000 km in length from west to east and hosts about 40,000 km² of ice bodies. In this study, we investigated the heavily glacierized CKNP region in Karakoram, Northern Pakistan (Figure 1). The CKNP region spreads over 13,000 km² and it was formed in 2009, with more than 40% of the area covered by glaciers. ICIMOD 2013 revealed more than 700 glaciers in the CKNP region with an area of 4632 km², which is

30% of the total glaciers in the Karakoram range of Pakistan. The CKNP hosts some of the largest Karakoram glaciers, i.e., Biafo, Panmah, and Baltoro. Glaciers in the CKNP region show variations in type, geometry, size, and surface condition (clean ice and debris-covered ice) [7,33]. The area belongs to Hunza and Shigar basins. The annual runoff of these basins is based on glaciers and snowmelt because they are at high elevations [33]. The study area generally depends on two climatic regimes: westerlies in winter and monsoons in summer. With the transitional position of the mighty Nanga Parbat (northwestern Himalaya range) in between, the monsoon wind interrupts a little precipitation and the western disturbance brings heavy precipitation to the Karakoram region [34]. Consequently, the CKNP region is usually affected by winter precipitation [5]. According to Bocchiola and Diolaiuti (2013), three climatic regions belong to Northern Pakistan and the CKNP region is included in the Northwest Karakoram climate. In this region, the average winter and irregular spring and summer rainfall increases from 150–500 mm at 1500–3000 m above mean sea level (MSL) to more than 1700 mm at 5500 MSL, and winter precipitation nourishes the glacier of the HKH region [7].

2. Materials and Methods

The flow diagram of this study is presented in Figure 2, describing the various methods used to achieve the objective of this study. The Landsat data was downloaded from the United States Geological Survey USGS (Available online: <https://earthexplorer.usgs.gov/> (accessed on 25 July 2021)) for the glacier inventory. We have extracted topographic parameters from ASTER GDEM. All the acquired satellite images were projected to the WGS (World Geodetic System) 1984 UTM (Universal Transverse Mercator) Zone 43N and the atmospheric correction was performed in the preprocessing step of the methodology using GIS. Later, the processed Landsat bands were used to apply the NDSI and slope threshold method for the glacier inventory; in addition, the area was separately calculated for each year to estimate the pattern of ice distribution. Glacier shapefiles obtained from the Randolph Glacier Inventory (RGI version 6) were used to mask the area of glaciers (Figure 1) [35]. The rainfall and temperature data from 1990 to 2020 for Skardu and Gilgit meteorological stations were obtained from the Pakistan Meteorological Department (PMD). Rainfall was considered for the winter season while temperature was considered for the summer season. Eventually, the maps and graphs were prepared from the extracted information.

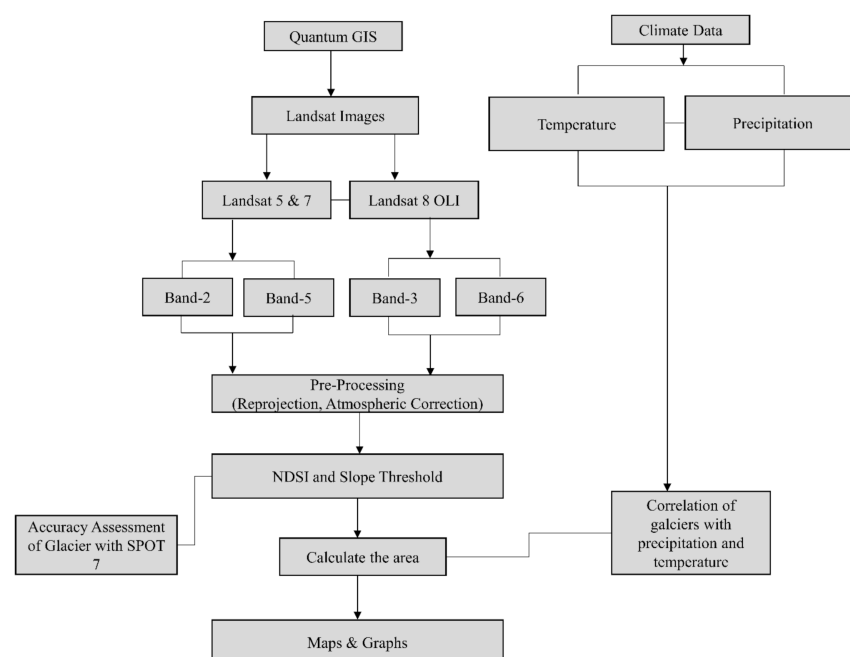


Figure 2. Flowchart of the study.

2.1. Satellite Imagery

To evaluate the cryosphere temporal changes in the CKNP region, we used Landsat. Landsat data is freely available and easily accessible. The multispectral Landsat has a long archive of satellite images that can be retrieved from the archive of the (USGS) (Available online: <https://earthexplorer.usgs.gov/> (25 July 2021)). For the accuracy assessment of the NDSI-classified glacier inventory, we purchased SPOT 7 images from Apollo Mapping Services.

2.1.1. SPOT

SPOT 7 orthorectified images were obtained for two different sites (Figure 3) within the study area to ascertain the accuracy of the glacier inventory obtained from the Landsat satellite because Landsat has 30 m of moderate resolution data. SPOT 6 and 7 satellites are the extension of the SPOT mission and launched successfully on 9 September 2012 and 7 June 2014. Both satellites have a spatial resolution of 1.5 m, pan-sharpened, and 6 m multispectral with a 60×60 km wide area image. SPOT images have also successfully been used for glacial studies in previous work [36,37].



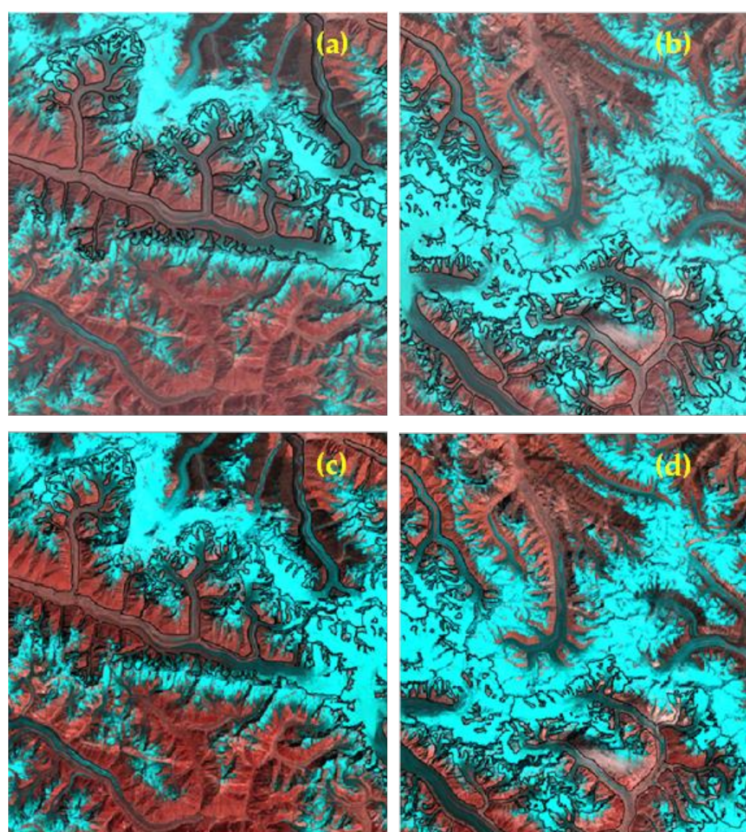
Figure 3. SPOT 7 satellite images with 1.5 m spatial resolution.

2.1.2. Landsat

Series of Landsat images are freely available at 30 m spatial and 16 days temporal resolution, respectively, which makes it an ideal choice for temporal cryosphere studies [38]. The satellite images were acquired for the month of August with the least cloud cover over the study area, which gives us a synoptic view of the study area from 1990 to 2020. (Table 1). The advantageous characteristic of Landsat images from Earth Explorer is that they are already in Level 1T format, thus there is no need for geo-reference and ortho-rectification. The detail of a scene, date of acquisition, sensor name, cloud cover, and spatial resolution of the images are presented in Table 1. The acquired satellite images are projected to WGS 1984 UTM Zone 43N. Burns and Nolin (2014) [30] stated that without atmospheric correction of satellite images, an erroneous calculation of debris-free glacier area are created. Thus, the satellite images were corrected atmospherically and topographically in QGIS using a semi-automatic classification tool (Figure 4). The digital numbers (DN) of the images were converted to the top of the atmosphere radiance (TOA) after radiometric correction.

Table 1. Remote sensing data was used for glacier mapping in this study.

| S. No | Acquisition Date | Sensor | Satellite | Spatial Resolution (m) | Cloud Cover |
|-------|------------------|--|------------|--|-------------|
| 1 | 7 August 1990 | Thematic Mapper (TM) | Landsat 5 | 30 | <10% |
| 2 | 29 August 2001 | Enhanced thematic mapper plus (ETM+) | Landsat 7 | 30 | 10% |
| 3 | 26 August 2009 | Thematic Mapper (TM) | Landsat 5 | 30 | <10% |
| 4 | 25 August 2020 | Operational land imager and thermal infrared sensor (OLI-TIRS) | Landsat 8 | 30 | <10% |
| 5 | 7 August 2020 | | SPOT 7 | 1.5 m (Pan-sharpen) 6 m Multispectral | 5% |
| 6 | November 2013 | | ASTER GDEM | 30 m | |

**Figure 4.** Landsat 8 OLI image with false color composite (a,b) before atmospheric correction and (c,d) after atmospheric correction. The image also shows much less cloud cover over the study area.

2.2. Digital Elevation Model (DEM)

In this study, high-resolution ASTER DEM (30 m resolution) was used and we downloaded version 2 of ASTER DEM from USGS (Available online: <https://earthexplorer.usgs.gov/> (accessed on 29 July 2021)) to estimate the spatial distribution of glaciers in the CKNP region according to elevation. To do this, we tried to identify the relationship between altitude and glacier changes, which is provenly appropriate for compiling the glacier topographic parameters [39]. The data was used to extract topographical parameters (aspect and elevation) to study glaciers.

2.3. NDSI Calculation

NDSI was proposed by Hall et al. (1995) [24] and has been used efficiently and frequently in many studies for glacial mass mapping [1,19,24,29,40]. It has been widely applied to the snow cover of mountainous regions due to its satisfactory results with detection in mountain shadows [27]. NDSI (Equation (1)) was chosen for this study to identify the snow cover by dividing the difference between the Green (Band 2 in L5 and L7, Band 3 in L8) and short-wave infrared bands (SWIR) (Band 5 in L5 and L7, Band 6 in L8). The NDSI value ranges from -1 to $+1$. Equation 1 was used to identify the snow cover. Various threshold values were used, e.g., ≥ 0.42 , ≥ 0.5 , and ≥ 0.6 , to accurately identify the snow distribution. Thus, in this study, a trial-and-error method [41] was used with an image classification tool in GIS, all of these values were tested, and the results were analyzed using the 1D histogram to evaluate the impact on snow cover mapping of shadowed areas. Eventually, the threshold of ≥ 0.40 was selected [24]. The same threshold value is reasonably proved in other studies [28,42,43].

$$\text{NDSI} = \frac{\text{Green}_{0.53} - \text{SWIR}_{1.65}}{\text{Green}_{0.53} + \text{SWIR}_{1.65}} \quad (1)$$

NDSI is effective to map the clean ice or glaciers but it creates erroneous results when it is applied to the debris-covered glacier due to its high spatial heterogeneity of the debris cover, which may mix ice and debris cover in optical imagery [31]. If the pixel is dominated by debris in spectral characteristics of imagery, it does not detect ice. In this case, manual delineation is usually possible but sometimes in-depth manual delineation is also not possible. Instead, a semi-automatic method that syndicates multispectral classification with a digital elevation model (slope) is useful for delineating clean ice and debris-covered glaciers [31]. Snow-accumulated areas in the Karakorum range are at a steep slope; however, debris cover is at a gentle slope ($< 8^\circ$) [16]. We used a terrain slope threshold of $\leq 12^\circ$ [18] in this study. Eventually, the glacier inventory was prepared by merging the NDSI-delineated and terrain-threshold-delineated boundaries.

2.4. Climatic Data

In this study, we assessed the impact of climate conditions on glacier dynamics. The temperature and precipitation data of Skardu and Gilgit meteorological stations were acquired from the Pakistan Meteorological Department (PMD) for the period from 1990–2020. Temperature was considered for the summer season (May–September) because glacier balance is a difference between accumulation and melting which, is usually known as remaining snow. We only used mean summer temperature in this study. Precipitation was considered for the winter season (Nov–Feb) because snowfall occurs in winter. The mean summer temperature ($^\circ\text{C}$) and mean winter precipitation (mm) data were analyzed with glacier inventory for the corresponding year, i.e., 1990, 2001, 2009, and 2020. We also correlated the clean ice with climatic data (temperature and precipitation) to see the relationship of ice with temperature and precipitation.

3. Results

3.1. Spatio-Temporal Changes in Glacier

The glaciers selected in this study (Khurdopin, Biafo, Hispar, Panmah, and Virjerab) show a retreating trend from 1990–2020 (Figures 5–7). The study results reveal that the ice had a decreasing trend from 1990–2020 for all glaciers; however, the debris-covered area consistently increased with time (Figure 5). These decreasing and increasing trends of ice and debris, respectively, can be easily observed in Figure 7a–d. The sub-images in Figure 7 show the enlarged view of circled areas for clear temporal changes. In Figure 8a–d, we understand that the glacier recession rate greatly depends on the weather condition.

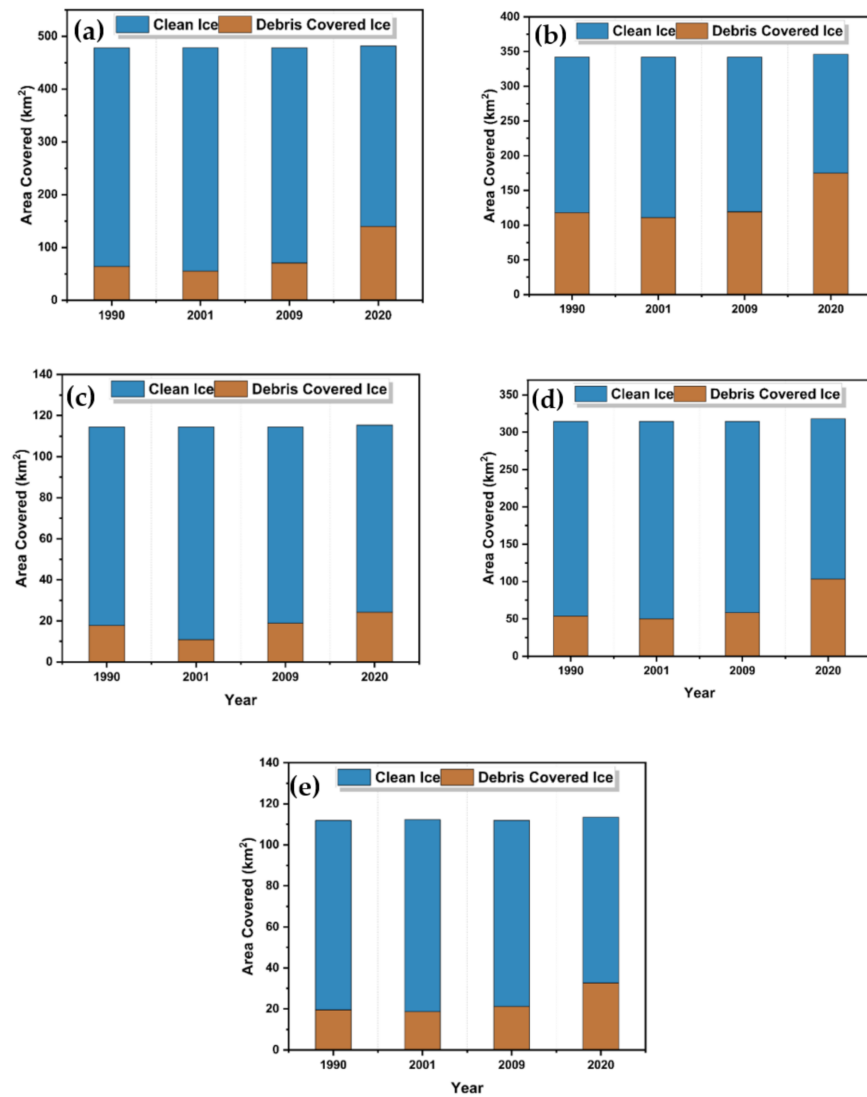


Figure 5. Glacier area changes from 1990–2020. (a) Biafo, (b) Hispar, (c) Khurdopin, (d) Panmah, and (e) Virjerab.

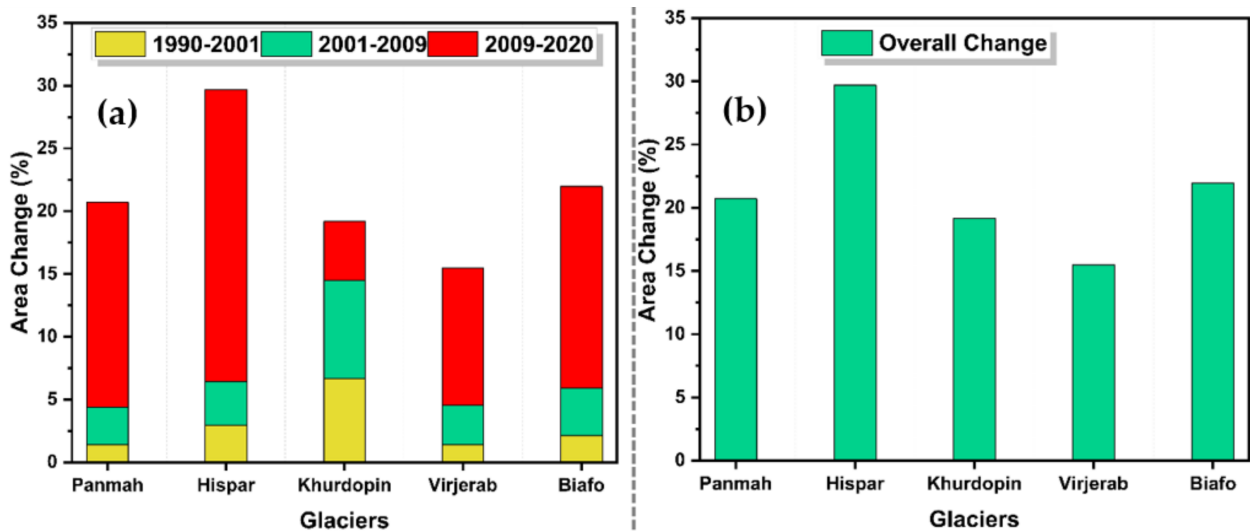


Figure 6. (a) Glacier area change for the periods from 1990–2001, 2001–2009, and 2009–2020. (b) Overall change from 1990–2020.

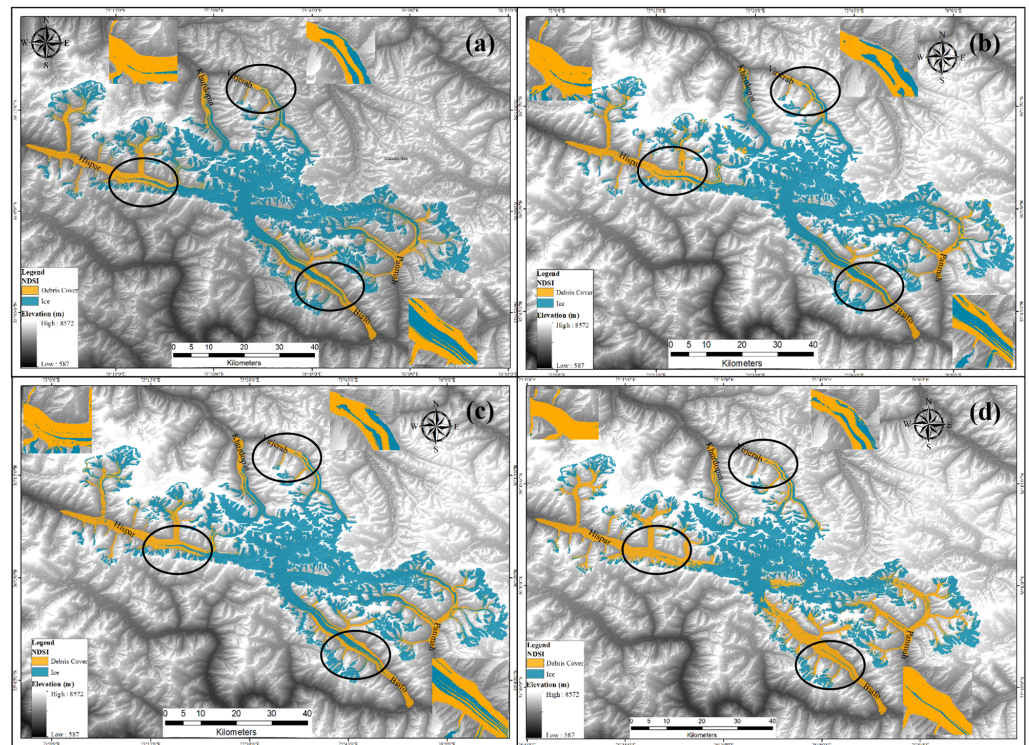


Figure 7. Glacier inventory of Central Karakoram National Park (CKNP) overlaid on ASTER 30-m DEM; (a) 1990, (b) 2001, (c) 2009, and (d) 2020. The yellow color shows debris-covered ice and the blue color shows clean ice. Encircled areas show the temporal variations in ice and debris-covered ice from 1990–2020 at various spots.

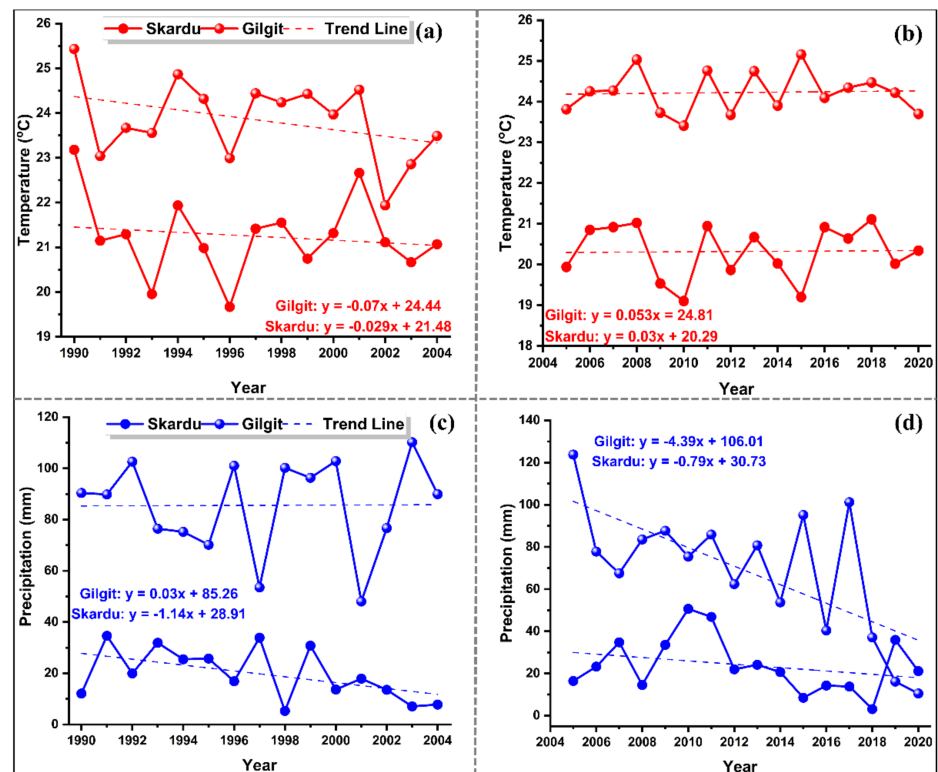


Figure 8. Climate variable (temperature and precipitation) time series; (a) temperature from 1990–2004, (b) temperature from 2005–2020, (c) precipitation from 1990–2004, and (d) precipitation from 2005–2020.

The glacier area increased in 2001, which may be due to the increased precipitation observed at the Gilgit meteorological station from 1990–2004 (Figure 8c). However, glaciers started retreating after 2001 and the glacier retreat rate between 2001 to 2009 for Panmah, Hispar, Khurdopin, Virjerab, and Biafo was 7.93, 7.93, 8.08, 2.94, and 15.84 km² with 0.99, 0.99, 1.01, 0.36, and 1.98 km²/year, respectively (Figure 5). An approximate 80–97% retreat rate was observed in the period from 2009–2020 for all glaciers [20,21] (Figures 5–7).

The areal distribution of ice significantly decreased; however, the debris cover area increased from 1990–2020 (Figure 5). The glacier snout variation was not observed because all glaciers are debris-covered, which is why it was difficult to observe it. However, it may be possible with high-resolution satellite images. Throughout the study period, the snout position of all glaciers was consistent due to a layer of debris; nevertheless, the area of ice inside the glacier melted.

3.2. Glacier's Inventory Accuracy Assessment

The Landsat-derived glacier inventory was evaluated with high-resolution SPOT 7 (1.5 m spatial resolution). An example of NDSI-classified ice and debris-covered ice patches is shown below in Figure 9a–h with referenced high-resolution image patches (Figure 9a''–h''). It can easily be seen that Landsat-derived NDSI-classified patches are in positive agreement with the high-resolution images that indicate the accuracy of Landsat and NDSI.

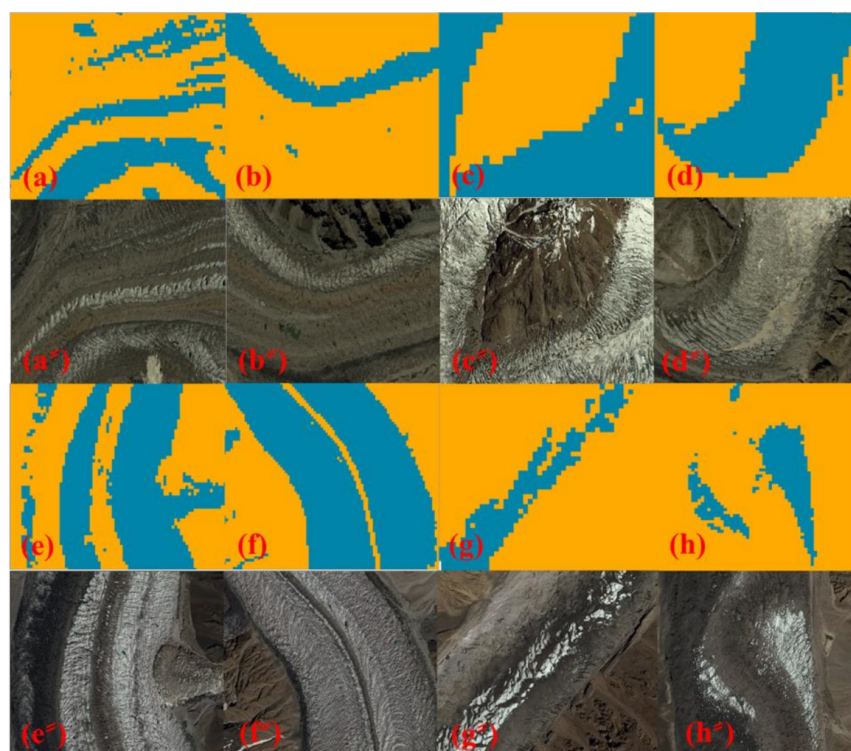


Figure 9. The images show the accuracy of NDSI compared to SPOT 7 high-resolution images; (a–h) NDSI classified patches from Landsat data, with blue color showing clean ice and yellow color showing debris-covered ice; (a''–h'') SPOT 7 high-resolution patches of the same area, with darker color showing the debris-covered ice and white color showing clean ice.

This observation also confirms that the 0.40 threshold performs very well, which is consistent with a previous study [44]. However, a recent study conducted by Tong et al. (2020) [40] concluded that the NDSI threshold is sensitive to snow depth, and seasonal and elevation changes. The same author also revealed that the NDSI threshold range between 0.2–0.4 results in somewhat similar mapping accuracy at various snow depths. The author suggested that seasonally and elevation-affected accuracy can be overcome by

using a 0.2 NDSI threshold value, which can increase to 3–10% accuracy for the months of January–March above 900 MSL.

We also calibrated the Landsat-derived NDSI images using high-resolution SPOT 7 images as shown in Figure 10. We converted the NDSI-classified images from raster to vector, overlaid the polygons on the satellite image, and inspected the NDSI outlines with the ones drawn on the SPOT 7 satellite images. We found very little difference between them, which is visible in Figure 10, and the difference between areas is also shown in Table 2 below. Thus, NDSI-derived glacier boundaries are acceptable, which is also found in other studies [18,30].

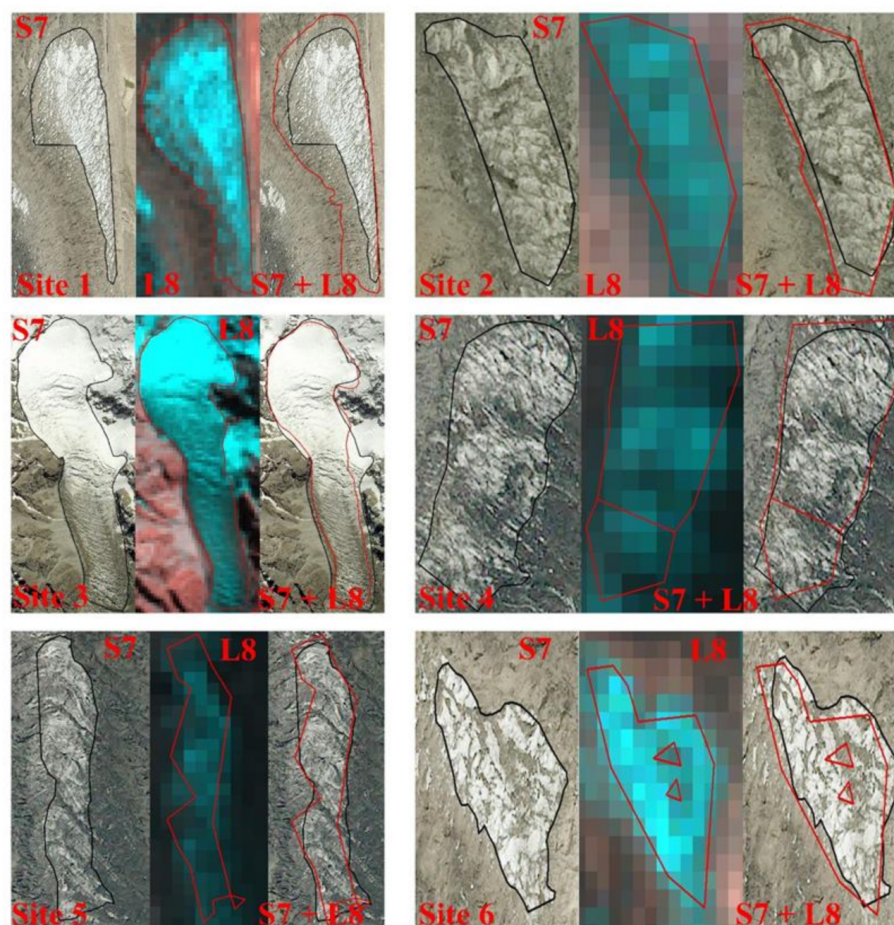


Figure 10. Comparison of images derived from Landsat 8 and SPOT 7 showing debris-covered ice and clean ice outlines at various spots. The black line shows outlines derived from SPOT 7 and the red line shows outlines derived from Landsat 8. S7: SPOT 7, L8: Landsat 8, Overlay: S7 + L8.

Table 2. Comparison between debris-covered ice and clean ice boundaries obtained from SPOT 7 and Landsat 8.

| | SPOT 7 (km ²) | Landsat 8 (km ²) | Difference (km ²) | Accuracy (%) |
|--------|---------------------------|------------------------------|-------------------------------|--------------|
| Site 1 | 1.68 | 1.45 | 0.23 | 86.31 |
| Site 2 | 0.42 | 0.69 | −0.27 | 60.87 |
| Site 3 | 0.06 | 0.07 | −0.01 | 85.71 |
| Site 4 | 0.08 | 0.07 | 0.01 | 87.50 |
| Site 5 | 0.04 | 0.05 | −0.01 | 80.00 |
| Site 6 | 0.066 | 0.062 | 0.004 | 93.95 |

3.3. Climatic Factors and Glacier Changes

To understand the relationship between climate factors and glacier changes, we used winter precipitation and summer temperature. Precipitation and temperature data for 31 years (1990–2020) were taken from the Pakistan Meteorological Department (PMD) (see Figure 1 for the location of meteorological stations). The climate pattern was estimated to build its relationship with glacier dynamics. The trend of mean summer temperature and mean winter precipitation was evaluated for Skardu and Gilgit meteorological stations, as both meteorological stations lie within the vicinity of the CKNP region. Linear regression analysis was performed using Microsoft Excel for the linear trend and the Mann–Kendall (MK) test was also used for trend estimation with a 95% significance level [45].

The MK trend test revealed that there was no significant trend in mean summer temperature and mean winter precipitation of Gilgit and Skardu stations; nonetheless, a mix of increasing and decreasing trends were observed in the precipitation and temperature data of Skardu and Gilgit meteorological stations. It was observed that precipitation at Gilgit and Skardu station increased by (0.22 mm/year) and decreased by (−1.40 mm/year), respectively, from 1990–2004. In the same period, the temperature at Gilgit and Skardu stations have a decreasing trend (−0.083 and −0.04 °C/year, respectively) (Table 3). Therefore, we can say that by observing the conditions of temperature and precipitation from 1990–2004, the clean ice area increased in 2001 because the temperature decreased at both stations while precipitation increased at Gilgit meteorological station. Linear regression analysis was also applied to both climatic variables and we observed that precipitation decreased at the Skardu meteorological station by −1.14 mm/year in the winter season from 1990–2004; on the contrary, for the same period, the rainfall at the Gilgit meteorological station showed an increasing trend of 0.03 mm/year (Figure 8c and Table 3). In addition, the linear regression results for mean summer temperature revealed a decreasing trend at both Skardu and Gilgit meteorological stations (−0.029 and −0.07 °C/year, respectively) (Figure 8a and Table 3).

Table 3. MK trend test (95% significance) and linear regression of winter precipitation and mean summer temperature from 1990–2004 and 2005–2020.

| Time Series | Linear Regression 1990–2004 | MK Test 1990–2004 | Linear Regression 2005–2020 | MK Test 2005–2020 |
|-------------------------|--------------------------------|----------------------|--------------------------------|----------------------|
| Precipitation (mm/year) | | | | |
| Skardu | −1.14 | −1.40 | −0.79 | −0.86 |
| Gilgit | 0.03 | 0.22 | −4.39 | −4.89 |
| Temperature (°C/year) | | | | |
| Skardu | −0.029 | −0.04 | 0.03 | 0.006 |
| Gilgit | −0.07 | −0.083 | 0.053 | 0.06 |

It was observed during analysis that about 80% of the glacier retreat was found during the period from 2009–2020 (Figure 7c,d), which is the highest of the total studied period. To clarify the pattern of the glacier recession, the MK test and linear regression methods were also applied for the specified period to reveal the trend. So, it was observed that rainfall at both (Skardu and Gilgit) meteorological stations showed a decreasing trend with values of −0.86 mm/year and −4.89 mm/year, respectively, which is in line with the linear regression trend of the precipitation for both Skardu and Gilgit meteorological stations, with −0.79 mm/year and −4.39 mm/year in the winter season during 2005–2020, respectively (Figure 8d and Table 3). The mean winter precipitation decreased rapidly compared to the previous period (1990–2004). In addition, the MK test was also applied to the mean summer temperature of both Skardu and Gilgit meteorological stations and results reveal that the temperature increased at a rate of 0.006 °C/year and 0.06 °C/year,

respectively. Similar results were also observed in linear regression analysis (Figure 8b and Table 3).

We further applied the Pearson correlation coefficient test to clean ice, temperature, and precipitation data (Table 4). It was noted that clean ice and temperature have a negative correlation for all glaciers but the correlation was not statistically significant; meanwhile, it was observed that precipitation and clean ice have a direct relationship. Therefore, we can say from these observations that snow accumulation happens in the winter season due to snowfall while snow melting in the summer season occurs due to a high summer temperature (Table 4).

Table 4. Pearson correlation of clean ice with temperature and precipitation.

| | Temperature | Precipitation |
|---------------------|-------------|---------------|
| Clean Ice Panmah | −0.935 | 0.802 |
| Clean Ice Hispar | −0.915 | 0.773 |
| Clean Ice Khurdopin | −0.846 | 0.835 |
| Clean Ice Virjerab | −0.953 | 0.836 |
| Clean Ice Biafo | −0.940 | 0.813 |

To evaluate the impact of climate variables (temperature and precipitation) on the glacier area, the glaciers were correlated with the impact of temperature and precipitation (Figure 11). It was observed that, with an increase in temperature, the area of the glacier retreated while increasing precipitation can nourish the snow and accumulate more snow. Therefore, we can see in Figure 11 that when the temperature decreased and precipitation increased, the glacier area increased in the year of 2001. However, as the temperature started rising again and precipitation fell, the glacier area continuously decreased between 2009 and 2020. That is why it was observed that around 80% of the glacier area retreated during the period from 2009–2020 (Figure 11a–e).

3.4. Area-Altitude Distribution

It was necessary to observe the glacier's area change distribution on elevation classes to understand the relationship between mountain elevation and ice distribution since the topographic parameter is responsible for glacier movement [39]. The glaciers of the CKNP region were mapped at elevation ranges from 3500 to 7745 MSL. More than 85% of the ice is distributed at the elevation range from 4500–6000 MSL (Figure 12 and Table 5). We observed that ice area decreased from 1990–2020 at the elevation ranges of 4500–5000, 5000–5500, and 5500–6000 at a rate of 65.90%, 15.78%, and 2.09%, respectively (Table 5).

Table 5. Glacier area and changes at different elevation zones in different years (1990–2020).

| Altitude | Glacier Area (km ²) | | | | Glacier Area Loss % | | |
|----------|---------------------------------|---------|---------|--------|---------------------|-----------|-----------|
| | 1990 | 2001 | 2009 | 2020 | 1990–2001 | 2001–2009 | 2009–2020 |
| MSL | 107.52 | 121.51 | 94.53 | 36.90 | 13.01 (+) | 22.20 (−) | 60.96 (−) |
| <4500 | 107.52 | 121.51 | 94.53 | 36.90 | 13.01 (+) | 22.20 (−) | 60.96 (−) |
| 5000 | 301.29 | 299.93 | 300.06 | 253.76 | 0.45 (−) | 0.04 (+) | 15.43 (−) |
| 5500 | 408.3 | 397.08 | 406.18 | 399.77 | 2.74 (−) | 2.20 (+) | 1.57 (−) |
| >5500 | 214.34 | 205.54 | 212.20 | 210.62 | 4.1 (−) | 3.24 (+) | 0.74 (−) |
| Total | 1031.46 | 1024.06 | 1012.97 | 901.06 | 0.71 (−) | 1.08 (−) | 11.04 (−) |

Note: The plus and minus signs represent increasing and decreasing mass balance.

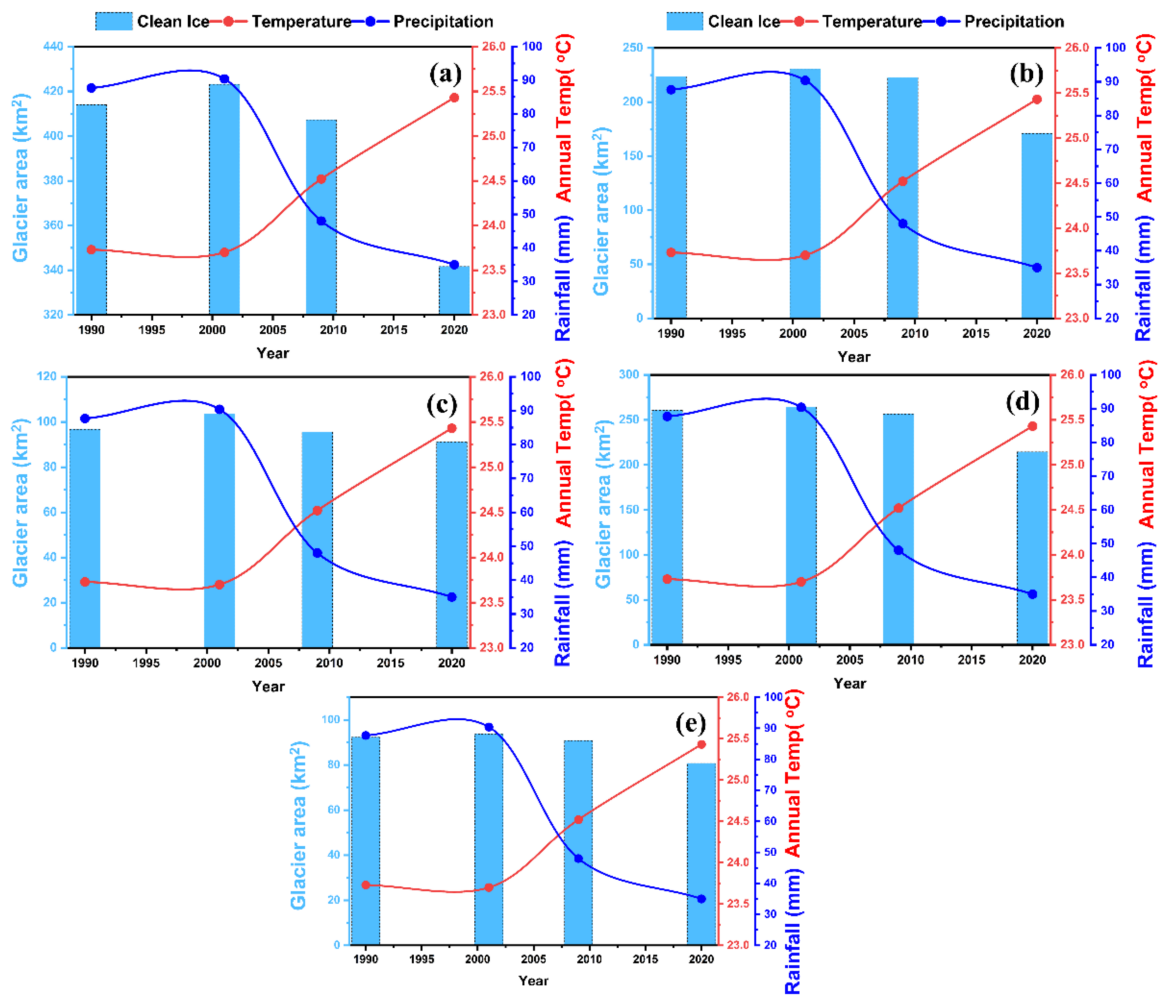


Figure 11. Correlation of glacier area with temperature and precipitation; (a) Biafo, (b) Hispar, (c) Khurdopin, (d) Panmah, (e) Virjerab. The vertical axis on the left-hand side show glacier area (km^2) while the right-hand side of the graph shows temperature ($^{\circ}\text{C}$) and precipitation (mm).

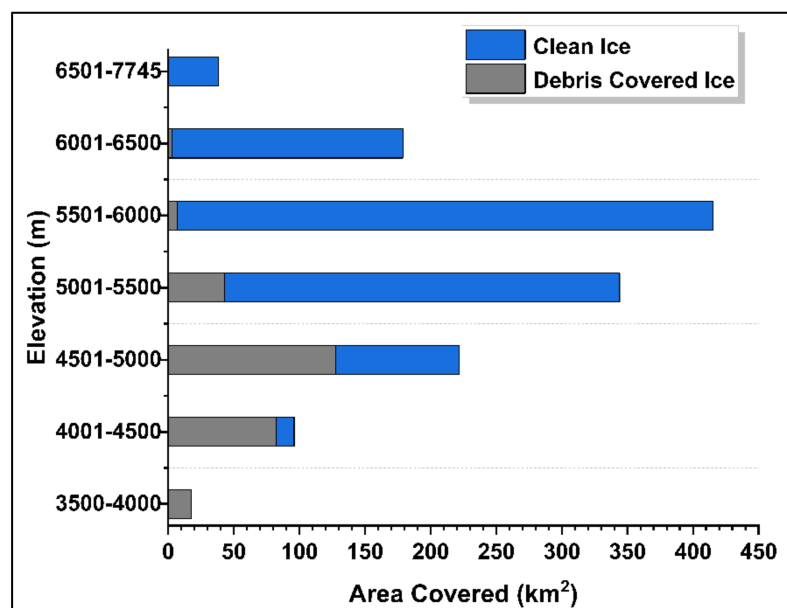


Figure 12. Distribution of ice and debris on different elevations.

Thus, this observation specifies that the ice area at a moderate to high elevation loses more area. The highest change in the ice is observed for the elevation level of less than 4500 MSL for the period from 2009–2020 (60.96%) followed by 4500–5000 MSL (15.43%) (Table 5). Moreover, supra-glacial lakes have been observed at an elevation level of less than 4500 MSL, which is related to a change in debris-covered ice and clean ice (Figure 13). However, no massive loss of ice area was found from 2000 through 2020 for the elevation level greater than 5500 MSL (Table 5).

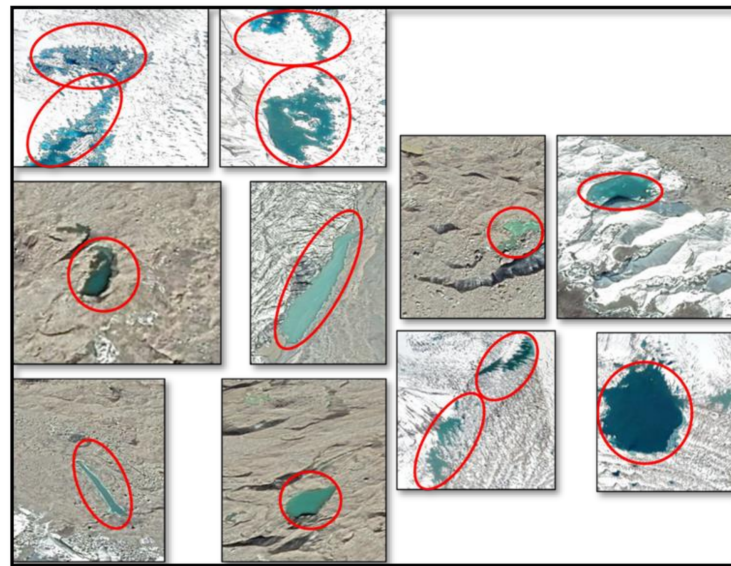


Figure 13. Supra-glacial lakes with debris-covered ice and clean ice from high-resolution Google Earth image, 2020. Red circles show supra-glacial lakes.

In this study, we observed that the northeast-facing slope lost maximum ice (26.04 km^2) during the period from 1990–2020, followed by the south (24.94 km^2) and southwest (21.72 km^2), and relatively minimum was lost in the north (12.62 km^2), followed by the west (16.07 km^2) (Figure 14a). On the contrary, the minimum amount of debris-covered ice increased on the north slope (12.5 km^2), followed by the west (15.9 km^2), and the highest was observed for the northeast slope (25.8 km^2), followed by the south (24.8 km^2) and southwest (21.6 km^2) (Figure 14b).

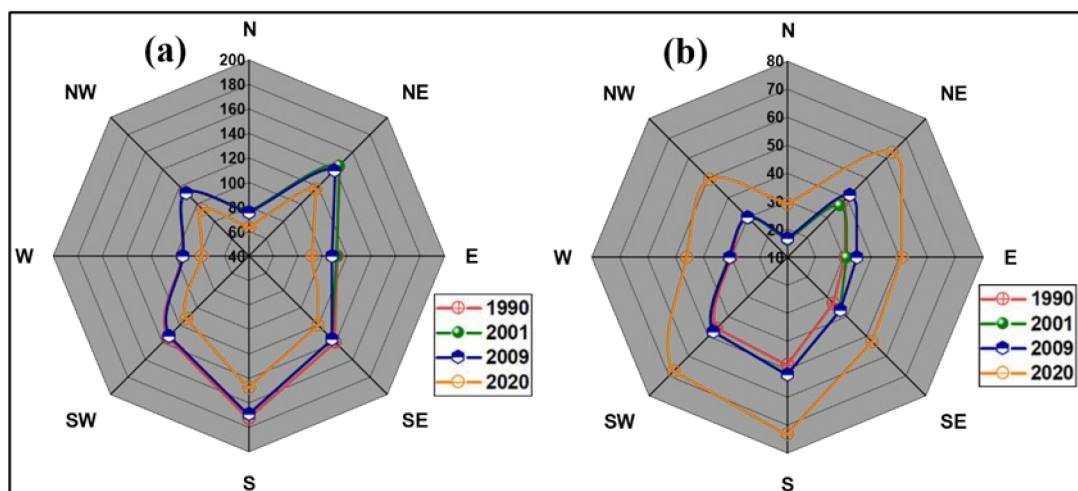


Figure 14. Debris and ice distribution on slope aspects (km^2); (a) area covered by ice and (b) area covered by debris at different slope aspects for the years 1990, 2001, 2009, and 2020.

4. Discussion

In the present study, we have evaluated the spatio-temporal distribution of the CKNP glaciers in the province of Gilgit Baltistan (GB), with the availability of archived Landsat spatio-temporal images. We found that the satellite data show clear phenomena of glacier changes from the period from 1990–2020 and revealed that it has been continually retreating. The findings of this study are comparable to some of the previous studies in the same region (Table 6) and around the globe, i.e., the Baltoro glacier in the HKH region [42], Tista basin, Sikkim Himalaya [20], Alps region [43,46], Hunza valley [18], and Alaska region [47].

Table 6. Comparison of the glaciers studied in this research with previous studies.

| Glaciers | Period | Present Study | Previous Studies | | References |
|-----------|-----------|---------------|------------------|--------------------------|----------------------------|
| | | Rate (%) | Rate (%) | Coverage km ² | |
| Panmah | | 1.48 | | | |
| Hispar | 1990–2018 | 1.7 | 1.35 | 245 | Mazhar et al. 2020 [19] |
| | 1977–2014 | | 0.17 | 398 | Shafique et al. 2018 [18] |
| Virjerab | | 0.37 | | | |
| Biafo | 1990–2000 | 2.33 | 0.7 | | Gilany and Iqbal 2016 [48] |
| Khurdopin | | 0.18 | | | |

The IPCC (2013) report perceived that the global temperature increased at a rate of 0.85 °C since 1980 and may reach 3.7 °C by end of the 21st century. Pepin et al. (2015) [49] revealed that a mountain's surface temperature is increasing more rapidly than the global average temperature. Correspondingly, the temperature of northern Pakistan will rise by 0.76 °C/decade for the period from 2011–2050 [50] and Raza et al. (2016) [51] also revealed the variation in day and night temperature. The authors also observed a positive change in the daily mean temperature of GB, which is in line with this study. This study revealed the decrease in precipitation and the increase in mean summer temperature for the reference years ultimately leading to melting of glaciers, which is consistent with the observation of Shafique et al. (2018) [18] for Hunza between 1977–2014.

In this study, area-altitude distribution provided perception into the interaction of the glaciers with various elevation zones. Notably, it was observed that almost 75% of the area on the valley floor is covered by debris-covered ice, which increased in the later years, and the observed increase due to the melting of ice results in the exposure of debris-covered ice [3]. In addition, it was apparent that more than 85% of ice lies in the elevation range of 4500–6000 MSL. However, over time, the area of ice has decreased in the same elevation range except for the year 2009. The changing pattern of ice area was observed due to the changes in precipitation for the particular year. It is to be noted that other studies by Minora et al. (2013 and 2016) [52,53] and Hussain et al. (2019) [54] found similar results compared to the present study. The melting of glaciers has a vast impact on water resources as it leads to water scarcity. Climate variables (temperature and precipitation) are the significant driving factors to disturbing the behavior of glaciers [20]. The present study provides a baseline investigation of glacier health for the last three decades that is useful for observing and predicting the future glacier dynamics and their interaction with climate.

5. Conclusions

In this study, a comprehensive picture of glaciers was drawn for the temporal period from 1990–2020 (31 years) in the CKNP region using ASTER DEM, and multi-temporal Landsat images with climate data were used to evaluate glacier dynamics. The remote sensing-based NDSI index and the DEM-based slope threshold method were used to delineate the clean ice and debris-covered ice, respectively. It was observed that the rate of glaciers varies spatially and temporally. It spatially varies because of the ice thickness

and distribution of debris-covered glaciers; on the other hand, it temporally varies due to variations in climatic variables. Some of the significant findings of this study include:

1. The glacier retreat in the CKNP region from 1990–2020 for Panmah, Hispar, Khurdopin, Virjerab, and Biafo was 46.05, 52.91, 5.63, 11.57, and 72.27 km² with 1.48, 1.70, 0.18, 0.37, and 2.33 km²/year, respectively.
2. The higher recession rate observed for the Biafo glacier is 2.33 km²/year, which is followed by Hispar (1.70 km²) and Panmah with a rate of 1.48 km²/year. The Khurdopin and Panmah glaciers have retreated 5.63 km² and 11.57 km² in the last 31 years (1990–2020).
3. From 1990–2001, the glaciers showed a minor advancing trend with 0.33, 0.62, 0.63, 0.12, and 0.82 km²/year for Panmah, Hispar, Khurdopin, Virjerab, and Biafo, respectively, due to increased precipitation at Gilgit station, and the temperature dropped at both stations.
4. In the studied time, almost 80% of the retreating trend was found between 2009–2020. This is possibly due to the dramatic decrease in precipitation of both Skardu and Gilgit meteorological stations with -0.79 mm/year and -4.39 mm/year, respectively, for the period from 2005–2020. In addition, it was also observed that the mean summer temperature increased at both stations at a rate of 0.03 °C/year and 0.053 °C/year, respectively.
5. The rate of glacier area retreat varies in different elevation zones: glaciers are receding at the elevation level of 4500–6000 m; however, the debris-covered ice at low elevation is advancing.
6. More than 75% of the area at the elevation level below 4000 MSL is covered by debris-covered ice.
7. Supra-glacial lakes have been observed below the elevation of 4500 MSL.
8. NDSI, thermal band, and Landsat satellite are very useful to estimate the spatio-temporal ice distribution.

A comprehensive evaluation of glaciers needs to be studied to better understand the state of glaciers. Future studies on regional climate prediction and its relationship with glaciers should be carried out to predict the glacier recession rate because meltwater from these glaciers is of great significance to the downstream region and the amount of water reduction and changes in glaciers can lead to water scarcity. Therefore, studies on glacier dynamics, water resource management, and hydrological planning can play a significant role in water security.

Author Contributions: M.F.U.M. and B.G.L.; conceptualization. M.F.U.M.; data acquisition, data curation, formal analysis, investigation, methodology, validation, visualization, and writing—original draft. B.G.L. and J.B.; writing—review and editing, and supervision. B.G.L.; project administration, resources, and funding acquisition. All authors have read and agreed to the published version of the manuscript.

Funding: This research was a part of the project titled “Jeju Sea Grant” funded by the Ministry of Oceans and Fisheries, South Korea.

Institutional Review Board Statement: Not applicable.

Informed Consent Statement: Not applicable.

Data Availability Statement: The dataset used in this study is available to the public at <https://earthexplorer.usgs.gov/> (accessed on 25 July 2021). However, the SPOT data were purchased and can be acquired from the corresponding author upon a reasonable request.

Acknowledgments: The authors acknowledge the United States Geological Survey (USGS) and National Aeronautics and Space Administration (NASA) for providing the Landsat data. The authors are thankful to NASA and the Ministry of Economy, Trade, and Industry (METI) for providing ASTER DEM free of cost for this study. The SPOT 7 images were purchased from Apollo Mapping.

The authors extend their acknowledgment to the Pakistan Meteorological Department (PMD) for providing the precipitation data.

Conflicts of Interest: The authors declare that the research was conducted in the absence of any commercial or financial relationships that could be construed as a potential conflict of interest.

References

1. Imran, M.; Ahmad, U. Geospatially analysing the dynamics of the Khurdopin Glacier surge using multispectral and temporal remote sensing and ground observations. *Nat. Hazards* **2021**, *108*, 847–866. [[CrossRef](#)]
2. Rowan, A.V.; Quincey, D.J.; Gibson, M.J.; Glasser, N.F.; Westoby, M.; Irvine-Fynn, T.; Porter, P.R.; Hambrey, M.J. The sustainability of water resources in High Mountain Asia in the context of recent and future glacier change. *Geol. Soc. Lond. Spéc. Publ.* **2018**, *462*, 189–204. [[CrossRef](#)]
3. Bajracharya, S.R.; Maharjan, S.B.; Shrestha, F. The status and decadal change of glaciers in Bhutan from the 1980s to 2010 based on satellite data. *Ann. Glaciol.* **2014**, *55*, 159–166. [[CrossRef](#)]
4. Gul, J.; Muhammad, S.; Liu, S.-Y.; Ullah, S.; Ahmad, S.; Hayat, H.; Tahir, A.A. Spatio-temporal changes in the six major glaciers of the Chitral River basin (Hindukush Region of Pakistan) between 2001 and 2018. *J. Mt. Sci.* **2020**, *17*, 572–587. [[CrossRef](#)]
5. Bookhagen, B.; Burbank, D.W. Toward a complete Himalayan hydrological budget: Spatiotemporal distribution of snowmelt and rainfall and their impact on river discharge. *J. Geophys. Res. Earth Surf.* **2010**, *115*, 1–25. [[CrossRef](#)]
6. Immerzeel, W.W.; van Beek, L.P.H.; Bierkens, M.F.P. Climate change will affect the Asian Water Towers. *Science* **2010**, *328*, 1382–1385. [[CrossRef](#)]
7. Bocchiola, D.; Diolaiuti, G. Recent (1980–2009) evidence of climate change in the upper Karakoram, Pakistan. *Theor. Appl. Clim.* **2013**, *113*, 611–641. [[CrossRef](#)]
8. Fowler, H.J.; Archer, D.R. Conflicting Signals of Climatic Change in the Upper Indus Basin. *J. Clim.* **2006**, *19*, 4276–4293. [[CrossRef](#)]
9. Hewitt, K. Tributary glacier surges: An exceptional concentration at Panmah Glacier, Karakoram Himalaya. *J. Glaciol.* **2007**, *53*, 181–188. [[CrossRef](#)]
10. Sabin, T.; Krishnan, R.; Vellore, R.; Priya, P.; Borgaonkar, H.; Singh, B.B.; Sagar, A. Climate change over the Himalayas. In *Assessment of Climate Change over the Indian Region*; Springer: Berlin/Heidelberg, Germany, 2020; pp. 207–222.
11. Krishnan, R.; Shrestha, A.B.; Ren, G.; Rajbhandari, R.; Saeed, S.; Sanjay, J.; Ren, Y. Unravelling Climate Change in the Hindu Kush Himalaya: Rapid Warming in the Mountains and Increasing Extremes. In *The Hindu Kush Himalaya Assessment: Mountains, Climate Change, Sustainability and People*; Wester, P., Mishra, A., Mukherji, A., Shrestha, A.B., Eds.; Springer International Publishing: Cham, Switzerland, 2019; pp. 57–97.
12. Sun, X.; Wang, K.; Kang, S.; Guo, J.; Zhang, G.; Huang, J.; Cong, Z.; Sun, S.; Zhang, Q. The role of melting alpine glaciers in mercury export and transport: An intensive sampling campaign in the Qugaqie Basin, inland Tibetan Plateau. *Environ. Pollut.* **2016**, *220*, 936–945. [[CrossRef](#)]
13. Bazai, N.A.; Cui, P.; Carling, P.A.; Wang, H.; Hassan, J.; Liu, D.; Zhang, G.; Jin, W. Increasing glacial lake outburst flood hazard in response to surge glaciers in the Karakoram. *Earth-Sci. Rev.* **2020**, *212*, 103432. [[CrossRef](#)]
14. Farinotti, D.; Immerzeel, W.W.; de Kok, R.J.; Quincey, D.J.; Dehecq, A. Manifestations and mechanisms of the Karakoram glacier Anomaly. *Nat. Geosci.* **2020**, *13*, 8–16. [[CrossRef](#)]
15. Forsythe, N.; Fowler, H.; Li, X.-F.; Blenkinsop, S.; Pritchard, D. Karakoram temperature and glacial melt driven by regional atmospheric circulation variability. *Nat. Clim. Chang.* **2017**, *7*, 664–670. [[CrossRef](#)]
16. Scherler, D.; Bookhagen, B.; Strecker, M.R. Spatially variable response of Himalayan glaciers to climate change affected by debris cover. *Nat. Geosci.* **2011**, *4*, 156–159. [[CrossRef](#)]
17. Kapnick, S.B.; Delworth, T.L.; Ashfaq, M.; Malyshev, S.; Milly, P.C.D. Snowfall less sensitive to warming in Karakoram than in Himalayas due to a unique seasonal cycle. *Nat. Geosci.* **2014**, *7*, 834–840. [[CrossRef](#)]
18. Shafique, M.; Faiz, B.; Bacha, A.S.; Ullah, S. Evaluating glacier dynamics using temporal remote sensing images: A case study of Hunza Valley, northern Pakistan. *Environ. Earth Sci.* **2018**, *77*, 162. [[CrossRef](#)]
19. Mazhar, N.; Amjad, D.; Javid, K.; Siddiqui, R.; Nawaz, M.A.; Butt, Z.S. Mapping Fluctuations of Hispar Glacier, Karakoram, using Normalized Difference Snow Index (NDSI) and Normalized Difference Principal Component Snow Index (NDSPCSI). *Int. J. Econ. Environ. Geol.* **2021**, *11*, 48–55. [[CrossRef](#)]
20. Chowdhury, A.; Sharma, M.C.; De, S.K.; Debnath, M. Glacier changes in the Chhombu Chhu Watershed of the Tista basin between 1975 and 2018, the Sikkim Himalaya, India. *Earth Syst. Sci. Data* **2021**, *13*, 2923–2944. [[CrossRef](#)]
21. Debnath, M.; Sharma, M.C.; Syiemlieh, H.J. Glacier Dynamics in Changme Khangpu Basin, Sikkim Himalaya, India, between 1975 and 2016. *Geosciences* **2019**, *9*, 259. [[CrossRef](#)]
22. Kehrwald, N.M.; Thompson, L.G.; Tandong, Y.; Mosley-Thompson, E.; Schotterer, U.; Alifimov, V.; Beer, J.; Eikenberg, J.; Davis, M.E. Mass loss on Himalayan glacier endangers water resources. *Geophys. Res. Lett.* **2008**, *35*, 1–6. [[CrossRef](#)]
23. Zhang, M.; Chen, F.; Tian, B.; Liang, D.; Yang, A. Characterization of Kyagar Glacier and Lake Outburst Floods in 2018 Based on Time-Series Sentinel-1A Data. *Water* **2020**, *12*, 184. [[CrossRef](#)]

24. Hall, D.K.; Benson, C.S.; Field, W.O. Changes of glaciers in Glacier Bay, Alaska, using ground and satellite measurements. *Phys. Geogr.* **1995**, *16*, 27–41. [[CrossRef](#)]
25. McFeeters, S.K. The use of the Normalized Difference Water Index (NDWI) in the delineation of open water features. *Int. J. Remote Sens.* **1996**, *17*, 1425–1432. [[CrossRef](#)]
26. Shukla, A.; Ali, I. A hierarchical knowledge-based classification for glacier terrain mapping: A case study from Kolahoi Glacier, Kashmir Himalaya. *Ann. Glaciol.* **2016**, *57*, 1–10. [[CrossRef](#)]
27. Kulkarni, A.V.; Singh, S.K.; Mathur, P.; Mishra, V.D. Algorithm to monitor snow cover using AWiFS data of RESOURCESAT-1 for the Himalayan region. *Int. J. Remote Sens.* **2006**, *27*, 2449–2457. [[CrossRef](#)]
28. Haq, M.A.; Jain, K.; Menon, K. Development of new thermal ratio index for snow/ice identification. *Int. J. Soft Comput. Eng.* **2012**, *1*, 2231–2307.
29. Bolch, T.; Buchroithner, M.; Pieczonka, T.; Kunert, A. Planimetric and volumetric glacier changes in the Khumbu Himal, Nepal, since 1962 using Corona, Landsat TM and ASTER data. *J. Glaciol.* **2008**, *54*, 592–600. [[CrossRef](#)]
30. Burns, P.; Nolin, A. Using atmospherically-corrected Landsat imagery to measure glacier area change in the Cordillera Blanca, Peru from 1987 to 2010. *Remote Sens. Environ.* **2014**, *140*, 165–178. [[CrossRef](#)]
31. Paul, F.; Huggel, C.; Kääb, A. Combining satellite multispectral image data and a digital elevation model for mapping debris-covered glaciers. *Remote Sens. Environ.* **2004**, *89*, 510–518. [[CrossRef](#)]
32. Pandey, A.; Sarkar, M.S.; Kumar, M.; Singh, G.; Lingwal, S.; Rawat, J.S. Retreat of Pindari glacier and detection of snout position using remote sensing technology. *Remote Sens. Appl. Soc. Environ.* **2018**, *11*, 64–69. [[CrossRef](#)]
33. Archer, D. Contrasting hydrological regimes in the upper Indus Basin. *J. Hydrol.* **2003**, *274*, 198–210. [[CrossRef](#)]
34. Nüsser, M.; Schmidt, S. Glacier changes on the Nanga Parbat 1856–2020: A multi-source retrospective analysis. *Sci. Total Environ.* **2021**, *785*, 147321. [[CrossRef](#)] [[PubMed](#)]
35. RGI. *A Dataset of Global Glacier Outlines: Version 6.0: Technical Report, Global Land Ice Measurements from Space*; CO, USA, 2017. Available online: <https://www.glims.org/RGI/> (accessed on 7 August 2022).
36. Kääb, A.; Leinss, S.; Gilbert, A.; Bühler, Y.; Gascoin, S.; Evans, S.G.; Bartelt, P.; Berthier, E.; Brun, F.; Chao, W.-A.; et al. Massive collapse of two glaciers in western Tibet in 2016 after surge-like instability. *Nat. Geosci.* **2018**, *11*, 114–120. [[CrossRef](#)]
37. Ragettli, S.; Bolch, T.; Pellicciotti, F. Heterogeneous glacier thinning patterns over the last 40 years in Langtang Himal, Nepal. *Cryosphere* **2016**, *10*, 2075–2097. [[CrossRef](#)]
38. Patel, A.; Prajapati, R.; Dharpure, J.K.; Mani, S.; Chauhan, D. Mapping and monitoring of glacier areal changes using multispectral and elevation data: A case study over Chhota-Shigri glacier. *Earth Sci. Inform.* **2019**, *12*, 489–499. [[CrossRef](#)]
39. Sevestre, H.; Benn, D.I. Climatic and geometric controls on the global distribution of surge-type glaciers: Implications for a unifying model of surging. *J. Glaciol.* **2015**, *61*, 646–662. [[CrossRef](#)]
40. Tong, R.; Parajka, J.; Komma, J.; Blöschl, G. Mapping snow cover from daily Collection 6 MODIS products over Austria. *J. Hydrol.* **2020**, *590*, 125548. [[CrossRef](#)]
41. Jabbar, A.; Othman, A.A.; Merkel, B.; Hasan, S.E. Change detection of glaciers and snow cover and temperature using remote sensing and GIS: A case study of the Upper Indus Basin, Pakistan. *Remote Sens. Appl. Soc. Environ.* **2020**, *18*, 100308. [[CrossRef](#)]
42. Abid, Z.; Zia, S. Mapping and analysis of Baltoto glacier and Shigar river. *Pak. Geogr. Rev.* **2019**, *74*, 20–32.
43. Sommer, C.; Malz, P.; Seehaus, T.C.; Lippl, S.; Zemp, M.; Braun, M.H. Rapid glacier retreat and downwasting throughout the European Alps in the early 21st century. *Nat. Commun.* **2020**, *11*, 3209. [[CrossRef](#)]
44. Härer, S.; Bernhardt, M.; Siebers, M.; Schulz, K. On the need for a time- and location-dependent estimation of the NDSI threshold value for reducing existing uncertainties in snow cover maps at different scales. *Cryosphere* **2018**, *12*, 1629–1642. [[CrossRef](#)]
45. Khan, A.A.; Zhao, Y.; Khan, J.; Rahman, G.; Rafiq, M.; Moazzam, M.F.U. Spatial and Temporal Analysis of Rainfall and Drought Condition in Southwest Xinjiang in Northwest China, Using Various Climate Indices. *Earth Syst. Environ.* **2021**, *5*, 1–16. [[CrossRef](#)]
46. Sigl, M.; Abram, N.J.; Gabrieli, J.; Jenk, T.M.; Osmont, D.; Schwikowski, M. 19th century glacier retreat in the Alps preceded the emergence of industrial black carbon deposition on high-alpine glaciers. *Cryosphere* **2018**, *12*, 3311–3331. [[CrossRef](#)]
47. Carlson, A.E.; Kilmer, Z.; Ziegler, L.B.; Stoner, J.S.; Wiles, G.C.; Starr, K.; Walczak, M.H.; Colgan, W.; Reyes, A.V.; Leydet, D.J.; et al. Recent retreat of Columbia Glacier, Alaska: Millennial context. *Geology* **2017**, *45*, 547–550. [[CrossRef](#)]
48. Gilany, S.N.A.; Iqbal, J. Geospatial analysis of glacial hazard prone areas of Shigar and Shayok basins. *Int. J. Innov. Appl. Stud.* **2016**, *14*, 623.
49. Pepin, N.; Bradley, R.S.; Diaz, H.F.; Baraer, M.; Caceres, E.B.; Forsythe, N.; Fowler, H.; Greenwood, G.; Hashmi, M.Z.; Liu, X.D.; et al. Elevation-dependent warming in mountain regions of the world. *Nat. Clim. Chang.* **2015**, *5*, 424–430. [[CrossRef](#)]
50. Chaudhry, Q.; Mahmood, A.; Rasul, G.; Afzaal, M. *Climate Change Indicators of Pakistan*; Pakistan Meteorological Department: Islamabad, Pakistan, 2009.
51. Raza, M.; Hussain, D.; Rasul, G. Climatic Variability and Linear Trend Models for the Six Major Regions of Gilgit-Baltistan, Pakistan: Climatic Variability and Linear Trend Models. *Proc. Pak. Acad. Sci. B. Life Environ. Sci.* **2016**, *53*, 129–136.
52. Minora, U.; Bocchiola, D.; D’Agata, C.; Maragno, D.; Mayer, C.; Lambrecht, A.; Diolaiuti, G.A. Glacier area stability in the Central Karakoram National Park (Pakistan) in 2001–2010: The “Karakoram Anomaly” in the spotlight. *Prog. Phys. Geogr.* **2016**, *40*, 629–660. [[CrossRef](#)]

53. Minora, U.; Bocchiola, D.; D'Agata, C.; Maragno, D.; Mayer, C.; Lambrecht, A.; Diolaiuti, G. 2001–2010 glacier changes in the Central Karakoram National Park: A contribution to evaluate the magnitude and rate of the “Karakoram anomaly”. *Cryosphere Discuss.* **2013**, *7*, 2891–2941.
54. Hussain, A.; Sagin, J.; Bekbayeva, A.; Abid, M. Climate Change and its Impact on Glaciers in Hindu Kush Region: A Case Study of Yarkhun Valley, Chitral Pakistan. In Proceedings of the 40th Asian Conference on Remote Sensing, Daejeon, Korea, 14–18 October 2019.